Opto-Electronic Advances

Supplementary information

April 2023, Vol. 6, No. 4

DOI: 10.29026/oea.2023.220105

Deep learning enhanced NIR-II volumetric imaging of whole mice vasculature

Sitong Wu[1,2†], Zhichao Yang[1,2†], Chenguang Ma[1†], Xun Zhang[1], Chao Mi[1], Jiajia Zhou[2], Zhiyong Guo[1,3*] and Dayong Jin[1,2,3*]

[1]UTS-SUStech Joint Research Centre for Biomedical Materials & Devices, Department of Biomedical Engineering, Southern University of Science and Technology, Shenzhen 518055, China; [2]Institute for Biomedical Materials & Devices, Faculty of Science, University of Technology Sydney, Ultimo, New South Wales 2007, Australia; [3]Guangdong Provincial Key Laboratory of Advanced Biomaterials, Southern University of Science and Technology, Shenzhen 518055, China.

[†]These authors contributed equally to this work.

*Correspondence: ZY Guo, E-mail: guozy@sustech.edu.cn; DY Jin, E-mail: Dayong.Jin@uts.edu.au

This file includes:

Supplementary information for this paper is available at https://doi.org/10.29026/oea.2023.220105

Methods

Reagents

Rare-earth oxides (RE: Yb, Er and Ce), polyacrylic acid (PAA; MW: 1,800), 1-(3-dimethylaminopropyl)-3-ethylcarbodiimide hydrochloride (EDC·HCl), $NOBF_4$ oleic acid (OA; 90%), oleylamine (OM; >80%), 1-octadecene (ODE; >90%) were purchased from Sigma-Aldrich. $RE(CF_3COO)_3$ (RE= Yb, Er and Ce) was prepared by the method previously described in the literature[S1]. CF_3COONa was purchased from Aladdin Ltd. Co., China. $Zn(CH_3COO)_2$ was purchased from Alfa Aesar. mPEG-NH_2 (MW: 5,000) was a commercial product from Nanocs.

Synthesis of $NaYbF_4$:Ce,Er,Zn (core) nanoparticles

In a typical procedure of synthesizing $NaYbF_4$: Er,Ce,Zn was prepared by the method previously described in the literature[S2]. In brief, 1 mmol CF_3COONa, 1 mmol $RE(CF_3COO)_3$ (RE: 96% Yb, 2% Er, 2% Ce) and 0.1 mmol $Zn(CH_3COO)_2$ were mixed solution of OA (10 mmol), OM (10 mmol), and ODE (20 mmol) in a three-necked flask at room temperature. Then the mixture was heated to 150 °C for 30 min under argon gas flow with vigorous magnetic stirring to evaporate all the residual water. Next, the solution was heated to 300 °C for 1.5 h under argon. After cooling to room temperature, the synthesized DSNPs were washed with cyclohexane/ethanol for three times and finally dispersed in 5 mL cyclohexane for further use.

Synthesis of $NaYbF_4$:Ce,Er,Zn@$NaYF_4$ (core-shell) nanoparticles

The core-shell structure is obtained via epitaxial growth on the core[S2]. In brief, 1 mmol CF_3COONa, $Y(CF_3COO)_3$ and the as-prepared core nanoparticles were mixed solution of OA (20 mmol) and ODE (20 mmol) in a three-necked flask at room temperature. Then the mixture was heated to 150 °C for 30 min under argon gas flow with vigorous magnetic stirring to evaporate all the residual water. Next, the solution was heated to 300 °C for 1.5 h under argon. After cooling to room temperature, the synthesized nanoparticles were washed with cyclohexane/ethanol for three times and finally dispersed in 5 mL cyclohexane for further use.

Surface modification of DSNPs

The synthesis of PAA and PEG coated DSNPs was carried out in a 2-step reaction[S3]. In the first step, oleic acid ligands of DSNPs ($NaYbF_4$:Ce,Er,Zn@$NaYF_4$) were removed using a nitrosonium tetrafluoroborate ($NOBF_4$). In brief, 5 mL of oleic acid coated DSNPs were dispersed in cyclohexane (5 mg/mL) and then mixed with 5 mL dichloromethane solution of $NOBF_4$ (0.01 M) at room temperature. After vigorous magnetic stirring for 20 min, the DSNPs were collected by centrifugation and re-dispersed in dimethy l-formamide (DMF). Next, 30 mg of PAA in 5 mL DMF was slowly added to the $NOBF_4$-treated DSNPs (6 mL, 5 mg/mL) with vigorous magnetic stirring for 12 h. In the second step, the carboxyl group of DSNPs-PAA was activated by EDC·HCl (30 mg), NHS (30 mg), and then 5 mL of mPEG-NH_2 (6 mg/mL) in MES buffer was slowly added to the mixture. After 2 h ultrasonic processing, dispersed in 5 mL water. The solution of DSNPs-PEG was dialyzed against water for 12 h (100 kDa) to remove excess mPEG-NH_2. The solution was concentrated by centrifugal filter (100 kDa) and dispersed in 625 μL saline solution.

Mouse handling

All BALB/c mice (male) were obtained from Guangdong Medical Laboratory Animal Center (Guangdong, China) and were raised in a specific pathogen-free (SPF) environment. All in vivo studies were performed with the permission of the Lab Animal Use Protocol of SUSTech. During the dynamic imaging, the mice was kept anesthetized with 2.5% isoflurane. For in vivo dynamic imaging, 200 μL solution of DSNPs-PEG (40 mg/mL) In saline solution was injected into one mice.

Time-gating strategy

We calculated the varies of luminous flux at the same speed with the change of duty cycle. The functions are shown as:

$$I = \frac{N}{T} \cdot \int_{t_1}^{t_2} P * W * (a \cdot \mathrm{e}^{-\frac{t}{\tau}+b})\mathrm{d}t \,, \tag{S1}$$

$$P = \frac{T}{N} - W - H \,, \tag{S2}$$

where I is the relative intensity of acquirement, N is the number of the chopper blades, T is the circle time of the chopper, t_1 to t_2 is the exposure time, P is the pulse width of the laser, W is the window size of the chopper, the exponential function is the lifetime decay of the DSNPs, H is the passing time of the time-gating hole. We can draw a curve with this function as shown in Fig. S1.

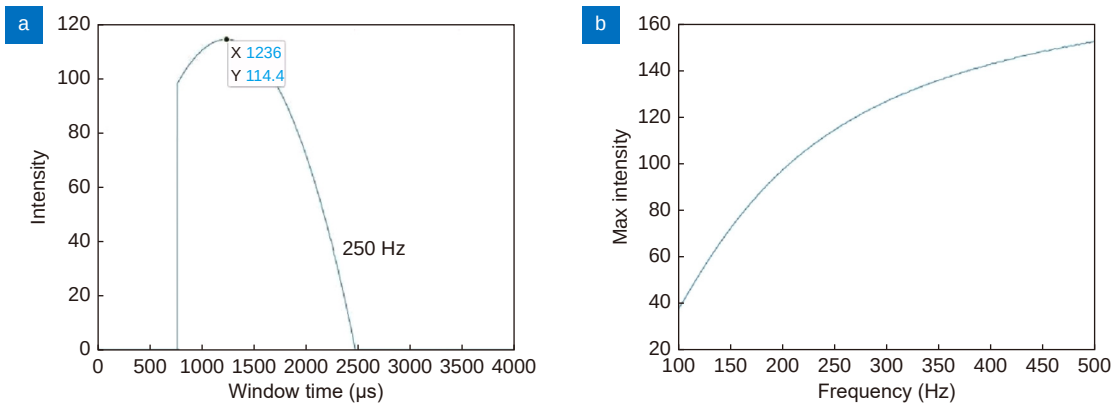

Fig. S1 | Variation of luminous flux with chopper parameters. (**a**) The luminous flux changes with the window width, at a frequency of 250 Hz. (**b**) Variation of maximum luminous flux at increasing frequency.

Comparison of photothermal effect

We compare the rising temperatures when the mice illuminated by CW mode light sheet and TG light sheet. At each average laser power, the mice is first cooled down to normal temperature, then illuminated by light sheet for 30 seconds. We test the maximum temperature using infrared thermal imager (ThermX pro) and calculate the rising temperatures as shown in Fig. S2.

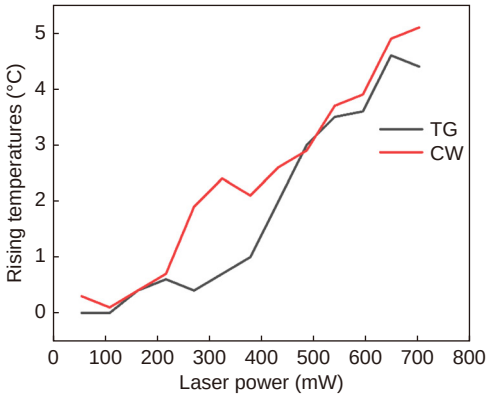

Fig. S2 | Rising temperatures of the mice illuminated by CW mode light sheet and TG light sheet.

Deep learning network

We use a DenseNet for vessel enhancement with network structure as shown in Fig. S3. We use a sliding window to generate training dataset from 15 pictures of wide field fluorescent imaging. We generate 10000 patches with pixel size of 15×15. The label is ***Ture*** if the center pixel of the patch is in the vessel part. We train this network on the GPU (NVIDIA RTX 2080ti). In the testing part, we use a sliding window to predict the testing pictures patch by patch.

Comparison of vessel enhancement algorithms

We compare Hessian-matrix based algorithm and our deep learning algorithm using a circle pattern with a gradient

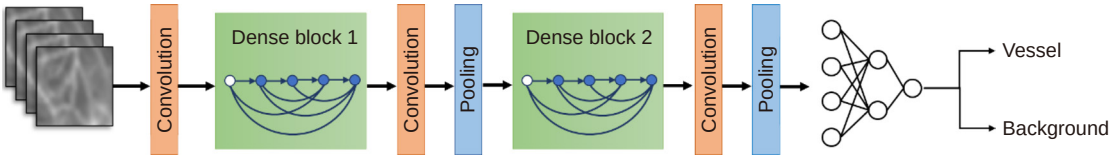

Fig. S3 | Deep learning network structure for vessel enhancement.

background. We also test the algorithms on this pattern with a SNR of 5 dB. In both of the comparisons, our algorithm shows better ability than the Hessian algorithm. The simulation results are in Fig. S4. The comparison results of fluorescent images are shown in Fig. S5.

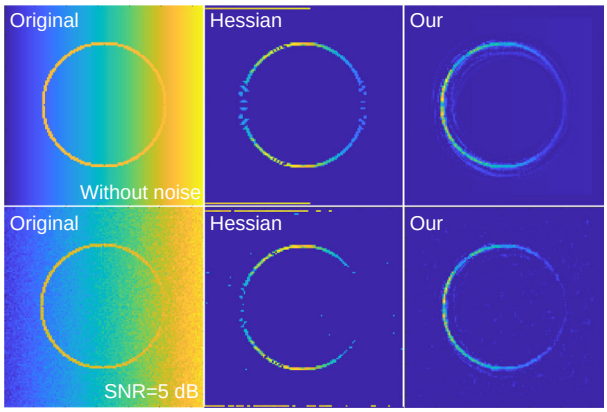

Fig. S4 | Comparison results of Hessian algorithm and out deep learning method.

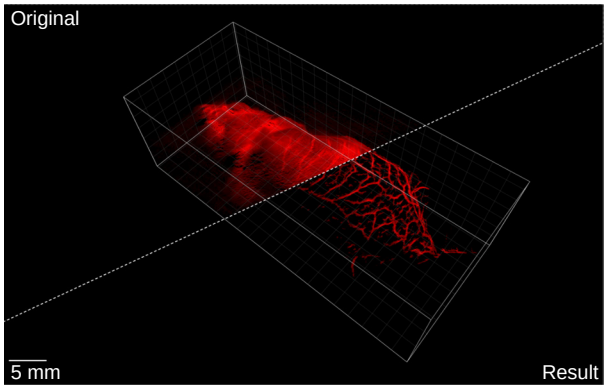

Fig. S5 | Comparison results of original image and our processed result.

Comparison of light sheet thickness

We compare the simulation results of light sheet thickness from 60 μm to 180 μm. We generate a 1000 μm× 1000 μm× 200 μm virtual phantom of blood vessel network. The results produced by different thicknesses of light sheets are shown in Fig. S6. It can be seen that the increased thickness of the light sheet affects the depth resolution.

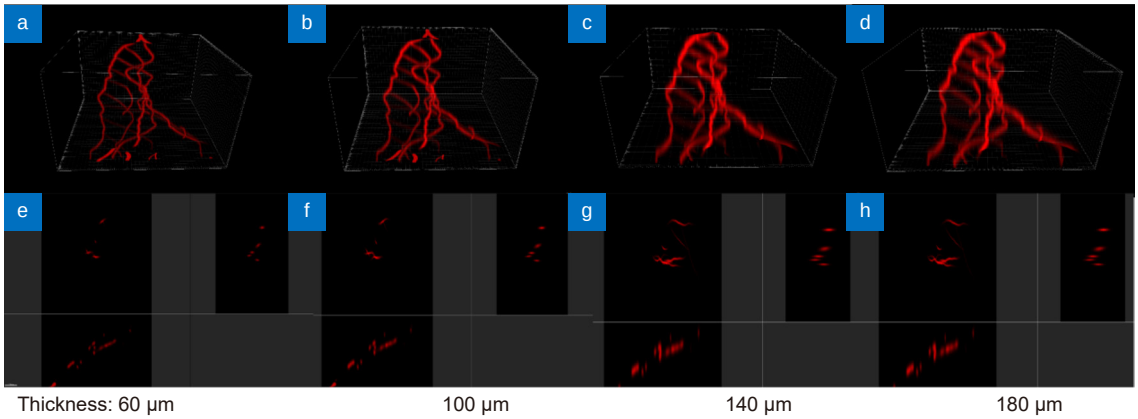

Fig. S6 | Comparison results of light sheet thickness from 60 μm to 180 μm in simulation.

References

S1. Roberts JE. Lanthanum and neodymium salts of trifluoroacetic acid. *J Am Chem Soc* **83**, 1087–1088 (1961).

S2. Zhong YT, Ma ZR, Wang FF, Wang X, Yang YJ et al. In vivo molecular imaging for immunotherapy using ultra-bright near-infrared-IIb rare-earth nanoparticles. *Nat Biotechnol* **37**, 1322–1331 (2019).

S3. Ai XZ, Ho CJH, Aw J, Attia ABE, Mu J et al. *In vivo* covalent cross-linking of photon-converted rare-earth nanostructures for tumour localization and theranostics. *Nat Commun* **7**, 10432 (2016).